2011 IEEE/RSJ International Conference on
Intelligent Robots and Systems
September 25-30, 2011. San Francisco, CA, USA

# Whole-Body Contact Manipulation Using Tactile Information for the Nursing-Care Assistant Robot RIBA

Toshiharu Mukai, Shinya Hirano, Morio Yoshida, Hiromichi Nakashima, Shijie Guo and Yoshikazu Hayakawa

*Abstract*— **In aging societies, there is a strong demand for robotics to tackle problems resulting from the aging population. We have developed a prototype nursing-care assistant robot, RIBA, which was designed to come in direct contact with patients and conduct physically challenging tasks. RIBA interacts with its object, typically a human, through multiple and distributed contact regions on its arms and body. To obtain information on such whole-body contact, RIBA has tactile sensors on a wide area of its arms. The regions where hard contact with the manipulated person may occur have almost flat surfaces, leading to surface contact involving a finite area, in order to reduce contact pressure and not to cause the person's pain. When controlling the position and orientation of the person, the relative positions and orientations of the distributed contacting surfaces should be preserved as far as possible to maintain stable contact and not to graze the person's skin. Preserving the force and the pressure pattern of each contact region using tactile feedback is also important to provide stable and comfortable human-robot physical interaction. In this paper, we propose a whole-body contact manipulation method using tactile information to meet these requirements.**

## I. INTRODUCTION

With the advent of an aging society, the demand for human-interactive robots that can help on-site caregivers by playing a role in nursing humans, particularly the elderly, is increasing. For this purpose, many robots have been proposed, for example, robots for feeding people who are paralyzed [1], mental commitment robots dedicated to improving mental health [2], and smart wheelchairs [3]. There are also wearing-type robots [4] that can support a caregiver's or patient's motion.

Tasks involving the transfer of a patient, such as lifting and moving a bedridden patient from a bed to a wheelchair and back, are among the most physically challenging tasks in nursing care. We have developed a prototype nursing-care assistant robot named RIBA (Robot for Interactive Body Assistance) [5] designed to conduct physically taxing tasks while in contact with a human as the manipulated object. RIBA has succeeded in transferring a human between a bed and a wheelchair, using human-type arms (Fig. 1). It has sufficient power to lift up a human weighing over 60 kg and soft smooth surfaces without projections. It interacts with the human as the object through distributed surface contact with a finite area on its outer shell. Information on the contacts is obtained by tactile sensors mounted on a wide area of its arms.

T. Mukai, S. Hirano, M. Yoshida and H. Nakashima are with RIKEN RTC, 2271-130, Anagahora, Shimoshidami, Moriyama-ku, Nagoya 463-0003, Japan {tosh,hirano,yoshida,nakas}@nagoya.riken.jp

S. Guo is with SR Laboratory, Tokai Rubber Industries, 1, Higashi 3-chome, Komaki, Aichi 485-8550, Japan shiketsu.kaku@tri.tokai.co.jp

Y. Hayakawa is with RIKEN RTC and Nagoya University, Furo-cho, Chikusa-ku, Nagoya 464-8601, Japan hayakawa@nuem.nagoya-u.ac.jp

Fig. 1. RIBA lifting a human in its arms.

The nursing-care tasks RIBA can potentially perform are not limited to sideways non-prehensile lifting as shown in Fig. 1. For example, patient transfer while supporting a human vertically in RIBA's arms may be possible. RIBA may also be used to assist standing and rehabilitation. To enable such tasks, we need methods of manipulating the position and orientation of the human as the object when the robot and human have multiple surface contact regions.

Manipulation that uses every surface of the robot is called whole-arm manipulation, on which considerable research, for example [6], [7], [8], has been conducted. In such research point contact is assumed and kinematics, dynamics, contact mode switching, and/or control are considered while sometimes allowing sliding or rolling of the contact points. When a robot manipulating an object on the floor is not fixed but physically interacts with the environment, which is typically the case of humanoid robots, different considerations from those for fixed arms or fingers are needed. Harada and Kaneko [9] dealt with this case and referred to such manipulation as whole body manipulation. They also assumed point contact in the manipulation.

In the situations we consider, where the manipulated object is a human, however, the robot and object must have distributed surface contact to ensure comfortable human-robot interaction. Furthermore, the contact should not produce a tangential force and the contacting surfaces must not slide to avoid grazing the human's skin. In their research on whole-body contact manipulation, Ohmura and Kuniyoshi [10] demonstrated the lifting of a box by their humanoid robot and pointed out the advantages of whole-body contact. Nozawa et al. [11] also demonstrated the lifting of a box by

TABLE I

Basic specifications of RIBA.

| | | |
|---|---|---|
| Dimensions | Width | 750 mm (when arms are folded) |
| | Depth | 840 mm |
| | Height | 1,400 mm |
| Weight inc. batteries | | 180 kg |
| D.O.F. | Head | 3 (only 1 in current use) |
| | Arm | 7 each |
| | Waist | 2 |
| | Cart | 3 (with 4 motored wheels) |
| Base movement | | Omnidirectional with omnidirectional wheels |
| Actuator type | | DC motor |
| Payload | | 63 kg (tested value) |
| Operation time | | 2 hour in standard use |
| Power | | NiMH batteries |
| Sensors | Vision | 2 cameras |
| | Audio | 2 microphones |
| | Tactile | Upper arm (128 pts. each) |
| | | Forearm (94 pts. each) |
| | | Hand (4 pts. each) |
| | | Shoulder pad (8 pts. each) |

their humanoid robot. The contact in their demonstrations was surface contact, but they did not deal with a trajectory generation method.

In this paper, we propose a whole-body contact manipulation method using tactile information suitable for robots designed to interact with a human. The method generates a joint trajectory that realizes the desired object trajectory while satisfying the conditions for comfortable contact. The required conditions may exceed the number of degrees of freedom (d.o.f.) of the robot; thus, the trajectories are determined by minimizing an evaluation function. To deal with modeling errors and control errors as well as external disturbances, feedback using tactile sensors is applied to adjust the trajectories.

## II. RIBA's Specifications

### A. Outline

RIBA is a prototype robot for enabling human-robot physical contact and conducting physically taxing tasks in real unstructured environments such as nursing-care facilities and hospitals. It has succeeded in lifting a human from a bed, placing a human on a bed, lifting a human from a wheelchair, putting a human down on a wheelchair, and moving with a human in its arms. Its basic specifications are summarized in Table I.

In the following subsections, we describe RIBA's specifications briefly, focusing on the features that are relevant to the whole-body contact manipulation in this paper. For more details, please refer to [5].

### B. Joint Configuration

RIBA and its joint configuration are shown in Fig. 2. The link between joints 3(10) and 4(11) is called the right(left) upper arm and that between joints 5(12) and 6(13) is called the right(left) forearm. Joints 4 and 11 enable elbow bending and 5 and 12 enable elbow rotation. When an object is manipulated by RIBA's arms and body, the number of joints used in the manipulation is 14, because the head and the wrists are not involved.

To provide a large power with compact motors, most joints in RIBA have high gear ratios (> 1000). As a result, the joints

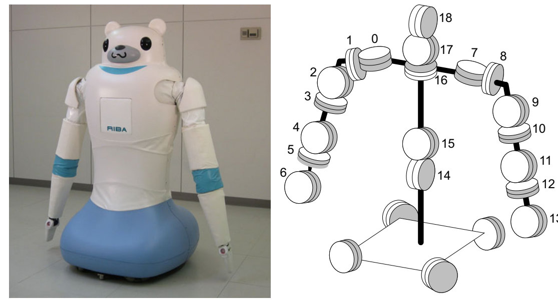


Fig. 2. RIBA and its joint configuration.

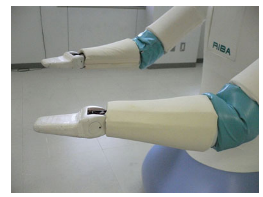

Fig. 3. Forearms, the shape of which fits the human back.

have no backdrivability. Each joint is position controlled by its local PID controller.

### C. Soft Surface and Forearm Shape That Fits a Human Body

To ensure safety in the case of unexpected contact, as well as the stability and comfort of the manipulated person, the entire body of RIBA including its joints is covered with soft materials such as polyurethane foam and a silicone elastomer. While lifting a human, as shown in Fig. 1, the weight is supported by distributed areas on the forearms, the upper arms, and the body. The forearms, which support a large proportion of the weight, have a slightly concave (semi-flat) surface that fits the human back, as shown in Fig. 3, to ensure comfortable contact for the lifted person. We call the side of the arms facing the body when taking the posture in Fig. 2 'inside' and the opposite side 'outside'. In nursing-care tasks, the inside of the arms contact with the patient.

### D. Information Processing System

RIBA has in it a distributed information-processing network consisting of the main PC (CPU: Intel CoreDuo, 2 GHz) and more than 20 local processing boards (CPU: Microchip dsPIC33F) to control the sensors or motors. The control loop periods of the tactile sensor controllers, the motor controllers, and the main PC are 4 ms, 1 ms, and 10 ms, respectively.

### E. Tactile Sensors

For the tactile sensors, we developed a flexible tactile sheet with $8 \times 8$ semiconductor pressure sensors and a readout circuit embedded in an elastic material [12]. This type of tactile sensor is mounted on the upper arms (Fig. 4) and forearms. Two tactile sheets are used to cover the inside and outside of each upper arm or forearm so as to cover the whole circumference. The tactile sheets on the forearm are

(a) Without cover (b) With cover

Fig. 4. Tactile sensors on the upper arm.

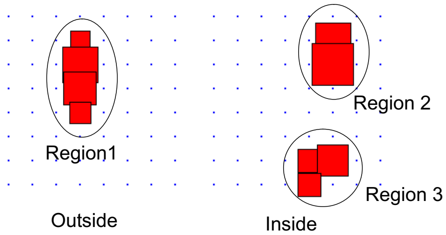


Fig. 5. Regions are extracted from the tactile sensor output and features are calculated for each region.

cut into a comblike shape with some of its teeth cut off to fit the complex shape of the forearm. The numbers of sensing elements on each upper arm and forearm are 128 and 94, respectively, and the spacing between elements is 21.5 mm.

The output of the tactile sensor is scanned and obtained by its local controller, which uses A/D converters to capture the resistive value of semiconductor pressure sensors used as sensing elements on the tactile sheet. The measurement range is from 0 to above 90 kPa and the measurement resolution of each sensing element is more than 5 bit. This enables the detection of a soft touch by a human finger and the weight of a human on the arms.

Two-dimensional tactile patterns on the tactile sensors are processed by their local controllers. The local controller first extracts separate regions consisting of neighboring active elements as shown in Fig. 5, then calculates feature values such as the total force and the position of the center of pressure for each region. The locally calculated features are sent to the main PC via the network in RIBA.

## III. Problem Formulation of Whole-body Contact Manipulation

The primary target of the manipulation in this paper is a human. A typical situation is shown in Fig. 6. The robot and human may have multiple distributed contact regions that are surface contact with finite area. We assume that the ideal human-robot spatial relationship such as the robot lifting or holding the human is given as the initial state by a certain method. The objective of the manipulation here is to control the position and orientation of the human as the object according to a given trajectory, while preserving the initial human-robot contact conditions as far as possible. We assume quasi-static motion and we do not consider active motion of the human. As allowable orientation trajectories, we consider only rotations that do not markedly change the object orientation relative to the gravitational field. Consequently, we can consider that the joint angles and the shape

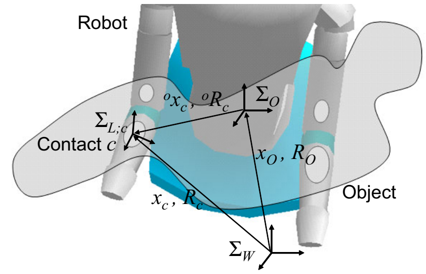


Fig. 6. Areas of contact between a robot and an object.

of the elastic parts of the human do not change, if the contact positions relative to the object do not change. As the contact conditions, we consider

i) the contact positions on the object surface (namely, human skin) and on the robot surface,

ii) the total force of each contact,

iii) the pressure distribution on each contact area.

If i) is not satisfied and the contacting surface slides, it may hurt the human by grazing the skin. If ii) is not satisfied, the robot may squeeze the held object when the force is too strong and drop it when the force is too weak. Condition iii) is necessary to prevent the contact becoming uneven and producing a concentrated force that may cause pain to the manipulated person.

To satisfy these conditions, we first generate a trajectory for the robot joints that preserves the positions and orientations of the contacting surfaces relative to the object. To determine the trajectory, we need to know the contacting positions on the robot, which can be obtained from the tactile sensors. Then, to deal with disturbances to the contact conditions, we apply tactile feedback. When there are multiple contact regions, the number of d.o.f. of the robot may be insufficient to satisfy the conditions. We thus introduce an evaluation function to balance the conditions.

Let $\Sigma_W$ and $\Sigma_O$ be the world coordinate frame and the object coordinate frame, respectively. The object coordinate frame $\Sigma_O$ is assigned to the object, and its position and orientation in the initial state can be arbitrarily determined. When the object has its inherent center in the structure, we set $\Sigma_O$ at this center, since we adjust the distance from $\Sigma_O$ in the tactile feedback. If we do not have information on the inherent center, we set $\Sigma_O$ at the mean of the contact positions in the initial state. The orientation of $\Sigma_O$ in the initial state is set to coincide with that of $\Sigma_W$ for simplicity. We describe the components of a vector or a rotation matrix with respect to $\Sigma_W$, unless otherwise stated. We use a rotation matrix to express the orientation of an object. Let $\tilde{\boldsymbol{x}}_O \in \mathbb{R}^3$ be the position vector of $\Sigma_O$ in the initial state, and $\boldsymbol{x}_O(t) \in \mathbb{R}^3$ and $R_O(t) \in \mathbb{R}^{3\times3}$ denote the position and orientation of the object at time $t$, respectively. By definition,

$$\boldsymbol{x}_O(0) = \tilde{\boldsymbol{x}}_O,\ R_O(0) = I, \tag{1}$$

where $I \in \mathbb{R}^{3\times3}$ is the identity matrix.

Let $C$ be the total number of contact regions and $c(c = 1,2,\dots,C)$ be the index used to express them. We assume that from tactile sensors we can obtain the coordinates $\boldsymbol{\xi}_c \in \mathbb{R}^2$

of the center of pressure and the normal force $f_c$ as the sum of the total pressure on each contact region $c$. Here, the components of $\boldsymbol{\xi}_c$ are expressed in the tactile sensor coordinate frame that is assigned to and spans the robot surface.

Let $\boldsymbol{q} = [q_1, q_2, \ldots, q_N]^T \in \mathbb{R}^N$ denote the robot joint angle vector, where $N$ is the total number of joints involved in the current manipulation and the joints are re-numbered from 1 to $N$. When the tactile sensor coordinates $\boldsymbol{\xi}_c$ and joint angle $\boldsymbol{q}$ are known, we can obtain the position $\boldsymbol{x}_c$ and rotation $R_c$ of the surface at $\boldsymbol{\xi}_c$ by calculating the forward kinematics. Here, we use the position and rotation of the local coordinate frame $\Sigma_{L;c}$ assigned to the surface at $\boldsymbol{\xi}_c$ as those of the surface. The rotation matrix of $\Sigma_{L;c}$ is used in the form of the discrepancy between the ideal and output orientations in the trajectory generation method, and the orientation relative to the surface has significance only when tactile feedback involving rotation is applied. Accordingly, we explain the method of determining the orientation in a later section.

We express the forward kinematic functions as

$$\boldsymbol{x}_c = \boldsymbol{T}_x(\boldsymbol{q};\boldsymbol{\xi}_c),\ R_c = T_R(\boldsymbol{q};\boldsymbol{\xi}_c). \tag{2}$$

From the position $\boldsymbol{x}_c(0) = \boldsymbol{T}_x(\boldsymbol{q}(0);\boldsymbol{\xi}_c(0))$ and rotation $R_c(0) = T_R(\boldsymbol{q}(0);\boldsymbol{\xi}_c(0))$ of the contact $c$ in the initial state, we can obtain the contact position and rotation with respect to the object coordinate frame $\Sigma_O$ as

$${}^O\boldsymbol{x}_c = \boldsymbol{x}_c(0) - \tilde{\boldsymbol{x}}_O,\ {}^OR_c = R_c(0). \tag{3}$$

The trajectory generation method should maintain the contact positions and orientations relative to $\Sigma_O$ as ${}^O\boldsymbol{x}_c$ and ${}^OR_c$, respectively, as far as possible while manipulating the object position $\boldsymbol{x}_O(t)$ and orientation $R_O(t)$. Furthermore, the position vector and rotation matrix are adjusted in the tactile feedback to maintain the contact state in the initial state.

## IV. Trajectory Generation Method

When the desired position and orientation of the manipulated object at time $t$ are given as $\boldsymbol{x}_O^d(t)$ and $R_O^d(t)$, respectively, the desired position and orientation of the contact $c$ that preserve the relation to the object center become

$$\begin{aligned} \boldsymbol{x}_c^d(t) &= \boldsymbol{x}_O^d(t) + R_O^d(t)^O\boldsymbol{x}_c, &(4)\\ R_c^d(t) &= R_O^d(t)^OR_c. &(5) \end{aligned}$$

We define a function for evaluating the deviations from the ideal positions and orientations and minimize it to deal with overconstrained cases. The evaluation function is

$$E = \frac{1}{2}\sum_c (w_c^x d_c(t)^2 + w_c^R \theta_c(t)^2) + \frac{1}{2}\sum_{i=1}^N w_{q;i}\dot{q}_i^2, \tag{6}$$

where $w_c^x$ and $w_c^R$ are the weighting factors for the deviations of the position and orientation of the contact $c$, respectively. The third term is introduced to restrict the change of $\boldsymbol{q}$ and $w_{q;i}$ is the weighting factor for $q_i$. We define the deviation of position as the norm of the difference between the desired and output (from the trajectory generation method) positions:

$$d_c(t) = \|\boldsymbol{x}_c(t) - \boldsymbol{x}_c^d(t)\|. \tag{7}$$

As the deviation of rotation, we use the axis-angle representation of rotation [13]. We define the absolute value of the equivalent angle of rotation from $R_c^d(t)$ to $R_c(t)$ as the deviation. To express this, we define the function to obtain the equivalent angle from rotation $R = (r_{ij})$ as

$$\theta = h(R) = \cos^{-1}\left(\frac{r_{11}+r_{22}+r_{33}-1}{2}\right), \tag{8}$$

where we limit the range of the function to $\theta \in [0,\pi)$. Then the deviation of rotation is expressed as

$$\theta_c(t) = h(R_c^d(t)^T R_c(t)). \tag{9}$$

We express the joint angle vector at time $t$, updated from the previous value, as

$$\boldsymbol{q}(t) = \boldsymbol{q}(t-1) + \Delta\boldsymbol{q}, \tag{10}$$

and obtain $\Delta\boldsymbol{q}$ that minimizes the evaluation function. We regard $E$, $d_c$, and $\theta_c$ as functions of $\Delta\boldsymbol{q}$ and define

$$\tilde{E}(\Delta\boldsymbol{q}) = \frac{1}{2}\left(\sum_c w_c^x d_c(\Delta\boldsymbol{q})^2 + \sum_c w_c^R \theta_c(\Delta\boldsymbol{q})^2 + \frac{1}{\Delta t^2}\Delta\boldsymbol{q}^T W_q \Delta\boldsymbol{q}\right), \tag{11}$$

where $\Delta t$ is the sampling period and

$$W_q = \mathrm{diag}\{w_{q;1}, w_{q;2}, \ldots, w_{q;N}\} \in \mathbb{R}^{N\times N}. \tag{12}$$

After applying the first-order approximation to $\tilde{E}$ under the assumption $\|\Delta\boldsymbol{q}\| \ll 1$ and setting the derivative of $\tilde{E}$ to $\mathbf{0}$, we obtain

$$\begin{aligned} \mathbf{0} &= \frac{\partial\tilde{E}}{\partial\Delta\boldsymbol{q}}\\ &= \sum_c w_c^x(\boldsymbol{x}_c(t-1) + J_c^x\Delta\boldsymbol{q} - \boldsymbol{x}_c^d(t))^T J_c^x\\ &+ \sum_c w_c^R(h(R_c^d(t)^T R_c(t-1)) + \boldsymbol{h}_c'\Delta\boldsymbol{q})\boldsymbol{h}_c' + W_q\Delta\boldsymbol{q}^T. \end{aligned} \tag{13}$$

Here, we regard $\boldsymbol{x}_c$ as a function of $\boldsymbol{q}$ in accordance with (2) and define its Jacobian matrix as

$$J_c^x = \left.\frac{\partial\boldsymbol{T}_x}{\partial\boldsymbol{q}}\right|_{\boldsymbol{q}(t-1);\xi_c} \in \mathbb{R}^{3\times N}. \tag{14}$$

We also define

$$\boldsymbol{h}_c' = \left.\frac{\partial h_c}{\partial\boldsymbol{q}}\right|_{\boldsymbol{q}(t-1);\xi_c} \in \mathbb{R}^{1\times N}, \tag{15}$$

which can be calculated as follows. From (8),

$$\begin{aligned} \boldsymbol{h}_c' &= -(1-(\frac{r_{11}+r_{22}+r_{33}-1}{2})^2)^{-1/2}\\ &\cdot\frac{1}{2}(\frac{\partial r_{11}}{\partial\boldsymbol{q}} + \frac{\partial r_{22}}{\partial\boldsymbol{q}} + \frac{\partial r_{33}}{\partial\boldsymbol{q}}). \end{aligned} \tag{16}$$

Because $R = R_c^d(t)^T R_c(t-1)$, we obtain

$$\begin{aligned} \frac{\partial r_{kk}}{\partial\boldsymbol{q}} &= \sum_{i=1}^3 r_{c;ik}^d(t)\frac{\partial r_{c;ik}}{\partial\boldsymbol{q}}(t-1)\\ &= \sum_{i=1}^3 r_{c;ik}^d(t)\left(\left.\frac{\partial T_R}{\partial\boldsymbol{q}}\right|_{\boldsymbol{q}(t-1);\xi_c}\right)_{ik}. \end{aligned} \tag{17}$$

After rearranging (13), we obtain

$$\begin{aligned}\Delta\boldsymbol{q} &= -\left(\sum_c\left(w_c^x(J_c^x)^TJ_c^x+w_c^R(\boldsymbol{h}_c')^T\boldsymbol{h}_c'\right)+\frac{1}{\Delta t^2}W_q\right)^{-1}\\ &\quad\cdot\left(\sum_c\left(w_c^x(J_c^x)^T(\boldsymbol{x}_c(t-1)-\boldsymbol{x}_c^d(t))\right.\right.\\ &\quad\left.\left.+w_c^Rh(R_c^d(t)^TR_c(t-1))(\boldsymbol{h}_c')^T\right)\right). \qquad (18)\end{aligned}$$

By setting a finite $w_{q;i}$, the inverse matrix becomes solvable even when the number of conditions is smaller than the number of the joints. When $\theta_c(t)=0$, the terms involved in the deviation of rotation of the contact $c$, namely, the terms with $\boldsymbol{h}_c'$, can be removed from the evaluation function because the condition on the orientation is already satisfied. This is helpful because $\boldsymbol{h}_c'$ becomes infinite when $\theta_c(t)=0$.

## V. Tactile Feedback

Because of modeling errors and control errors as well as external disturbances, the contact conditions may change, even when the joint angles obtained in the previous section are used as the reference values for position control. We apply tactile feedback to deal with such disturbances.

Each contact region has 6 d.o.f. (position and orientation), but in most cases it is difficult to adjust all of them using the tactile sensor output. Actually, the tactile sensors on RIBA can detect only the pressure (namely, normal stress) distribution on its surface, although by processing the pressure pattern over time, additional information can be estimated. In the tactile feedback in this paper, we change the contact positions by adjusting the length of ${}^O\boldsymbol{x}_c$ depending on the force on each contact to satisfy contact condition ii). We also apply an additional rotation to ${}^OR_c$ to satisfy contact condition iii), where we use the displacement of the center of pressure from the initial state.

In the adjustment of the length of ${}^O\boldsymbol{x}_c$, we define $s_c^x$ as the adjustment parameter of the contact $c$ and calculate a new ${}^O\boldsymbol{x}_c$ (expressed as ${}^O\boldsymbol{x}_c^{\text{new}}$) from the original ${}^O\boldsymbol{x}_c$ (expressed as ${}^O\boldsymbol{x}_c^{\text{org}}$) using the impedance control method to obtain smooth response as

$$M_c^x\ddot{s}_c^x+D_c^x\dot{s}_c^x+K_c^xs_c^x=f_c(t)-f_c(0), \qquad (19)$$

$${}^O\boldsymbol{x}_c^{\text{new}}={}^O\boldsymbol{x}_c^{\text{org}}+s_c^x\frac{{}^O\boldsymbol{x}_c^{\text{org}}}{\|{}^O\boldsymbol{x}_c^{\text{org}}\|}. \qquad (20)$$

Here, we define the positive direction of the normal force $f_c(t)$ so that the point at the contact $c$ moves away from the object surface. The constants $M_c^x, D_c^x$, and $K_c^x$ are virtual inertia, viscosity, and stiffness, respectively, which are determined to obtain a desirable response.

The additional rotation is applied to preserve the stable contact given as the initial state and to prevent partial uneven contact. When the contact $c$ becomes partial, the center of pressure $\boldsymbol{\xi}_c(t)$ moves from the initial position $\boldsymbol{\xi}_c(0)$. We apply the additional rotation to maintain $\boldsymbol{\xi}_c(t)$ close to the initial position.

We assume that the tactile sensor coordinate frame is orthogonal in the vicinity of the contact position $\boldsymbol{\xi}_c(0)$. If it is not orthogonal, we re-establish the coordinate frame to make it orthogonal. Let $\boldsymbol{e}_{c;i}\in\mathbb{R}^3 (i=1,2)$ be the tangential vectors at $\boldsymbol{\xi}_c(0)$ along the $\xi_{c;i}$-coordinate axis, as shown in Fig. 7.

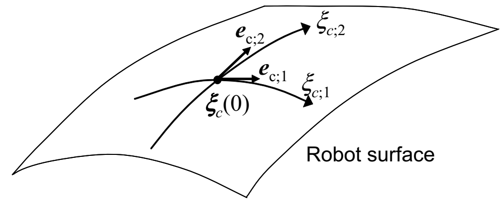


Fig. 7. Robot surface and its coordinate frame.

To maintain $\boldsymbol{\xi}_c(t)$ close to $\boldsymbol{\xi}_c(0)$, the additional rotation is determined from their difference $\boldsymbol{\xi}_c(t)-\boldsymbol{\xi}_c(0)$. We express the components of the additional rotation matrix with respect to the local coordinate frame $\Sigma_{L;c}$ that has its origin at $\boldsymbol{\xi}_c(0)$ and consists of axes $\boldsymbol{e}_{c;1}$, $\boldsymbol{e}_{c;2}$, and $\boldsymbol{e}_{c;1}\times\boldsymbol{e}_{c;2}$, where $\times$ denotes the outer product. To obtain a desirable response property, we prepare an adjustment parameter vector $\boldsymbol{\alpha}_c\in\mathbb{R}^2$ that is subject to an impedance control equation for smooth response

$$M_c^R\ddot{\boldsymbol{\alpha}}_c+D_c^R\dot{\boldsymbol{\alpha}}_c+K_c^R\boldsymbol{\alpha}_c=\boldsymbol{\xi}_c(t)-\boldsymbol{\xi}_c(0), \qquad (21)$$

where $M_c^R, D_c^R$, and $K_c^R$ are virtual inertia, viscosity, and stiffness, respectively, and use it to determine the additional rotation. As the axis of the additional rotation, we define the unit tangential vector $\boldsymbol{k}_c(t)$ at $\boldsymbol{\xi}_c(0)$ orthogonal to $\alpha_{c;1}(t)\boldsymbol{e}_{c;1}+\alpha_{c;2}(t)\boldsymbol{e}_{c;2}$. The components of $\boldsymbol{k}_c(t)$ are expressed in $\Sigma_{L;c}$. The direction of $\boldsymbol{k}_c(t)$ is determined so that positive rotation about $\boldsymbol{k}_c(t)$ moves the point at the tactile sensor coordinates $\boldsymbol{\alpha}_c(t)$ away from the object surface. We also determine the rotation angle about $\boldsymbol{k}_c(t)$ as $\phi_c=\|\alpha_c\|$. Then the additional rotation becomes

$$\text{Rot}(\boldsymbol{k}_c,\phi_c), \qquad (22)$$

where $\text{Rot}(\boldsymbol{k},\phi)$ expresses the rotation matrix of angle $\phi$ about $\boldsymbol{k}$. The new ${}^OR_c$ (expressed as ${}^OR_c^{\text{new}}$) is obtained from the original ${}^OR_c$ (expressed as ${}^OR_c^{\text{org}}$) using

$${}^OR_c^{\text{new}}={}^OR_c^{\text{org}}\text{Rot}(\boldsymbol{k}_c,\phi_c). \qquad (23)$$

## VI. Experiments

### A. Generated Trajectory

We conducted experiments on trajectory generation in an overconstrained situation. We assumed that the manipulated object was in contact with the right upper arm, the left upper arm, the right forearm, and the left forearm at the center of the inside of each arm, and that the object position (the mean of the contact positions) was moved 0.1 m in the $x$-direction (sideways to the left) from the initial posture shown in Fig. 8. We set their contact indexes $c$ as 1, 2, 3, and 4, respectively. The weight factors in the evaluation function were set as $(w_1^x,w_2^x,w_3^x,w_4^x)=(0.3,0.3,1.0,1.0)$, $(w_1^R,w_2^R,w_3^R,w_4^R)=(0.05,0.05,0.2,0.2)$, and $w_{q;i}=10^{-4}$ $(i=1,2,\ldots,14)$.

The results are shown in Fig. 9, where the top graph shows the object position displacement and the evaluation function, and the middle and bottom graphs show the transitions of $d_c(t)$ and $\theta_c(t)$, respectively. Because the total number of

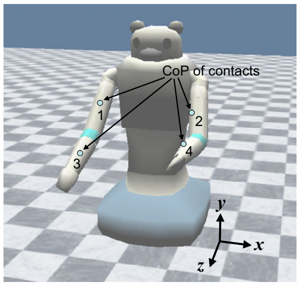


Fig. 8. RIBA's posture and contact positions in the initial state.

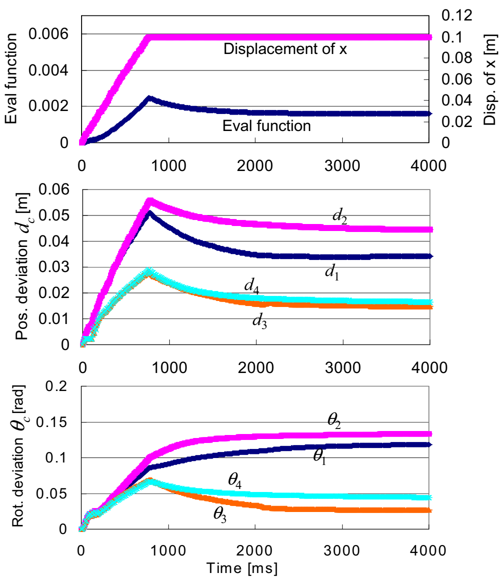


Fig. 9. Transition of the displacement, evaluation function, and deviations.

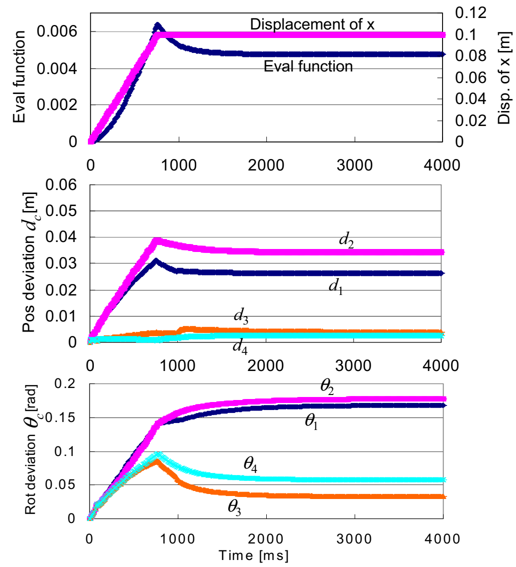


Fig. 10. Graphs showing comparison when the weight factors for position were increased.

Fig. 11. RIBA holding a cylinder in its arms.

d.o.f. of the contacts is 24 and is larger than 14, which is the number of joints involved in the manipulation, the evaluation function is overconstrained and cannot become 0. The deviations of the forearms are smaller than those of the upper arms, because we set larger weighting factors for the forearms than for the upper arms.

To observe the effect of changes in weighting factors, we next set larger weighting factors $(w_1^x, w_2^x, w_3^x, w_4^x) = (3, 3, 10, 10)$ for the deviations of position, while the other factors had the same values as before. The results are shown in Fig. 10, where the deviations of position are smaller than those in Fig. 9, while the deviations of rotation become larger owing to their trade-off relationship.

*B. Sensor Feedback*

To observe the effect of sensor feedback, we conducted experiments using RIBA. We chose the initial state in which RIBA was holding a cylindrical object covered with an elastic sheet between its forearms (Fig. 11), and moved the object 0.1 m in the $x$-direction. We use the indexes $c = 1$ and 2 for the contact on the right and left forearms, respectively. Although the final target of our manipulation is a human, we selected an inanimate object in the experiments in this paper, which may have been uncomfortable or dangerous to a human and thus should not be applied from the viewpoint of research ethics. Regarding repeatability and objectivity, experiments with an inanimate object are also preferable. The diameter of the cylinder was 140 mm and the thickness of the elastic sheet was 10 mm. The distance 0.1 m was selected because it is the quantity with which the robot cannot keep the object without sensor feedback. The constants in (19) and (21), tentatively determined for this experiment, are summarized in Table II.

First, we conducted experiments on the feedback of contact position to satisfy contact condition ii). The feedback of contact rotation was deactivated in these experiments. The results are shown in Fig. 12, where the top and middle graphs show the normal forces $f_c$ on the left and right forearms with and without sensor feedback, respectively, and the bottom graph shows the resulting $s_c^x$. In the experiment without sensor feedback, the normal forces changed markedly and the held object was dropped, while with sensor feedback, the changes in force were suppressed.

Next, we conducted experiments on the feedback of contact rotation to satisfy contact condition iii). The feedback of

TABLE II

CONSTANTS IN FEEDBACK CALCULATION.

| Symbol | $M_c^x$ | $D_c^x$ | $K_c^x$ | $M_c^R$ | $D_c^R$ | $K_c^R$ |
|---|---|---|---|---|---|---|
| Value | 545 | 1090 | 2725 | 0.0043 | 0.143 | 0.108 |
| Unit | Ns$^2$ | Ns | N | ms$^2$ | ms | m |

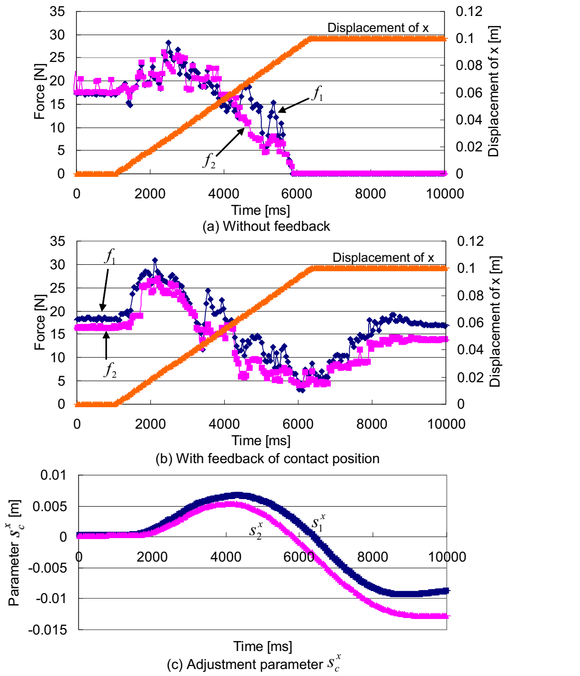


Fig. 12. Force $f_c$ and adjustment parameter $s_c^x$ on the forearms with and without feedback of the contact position.

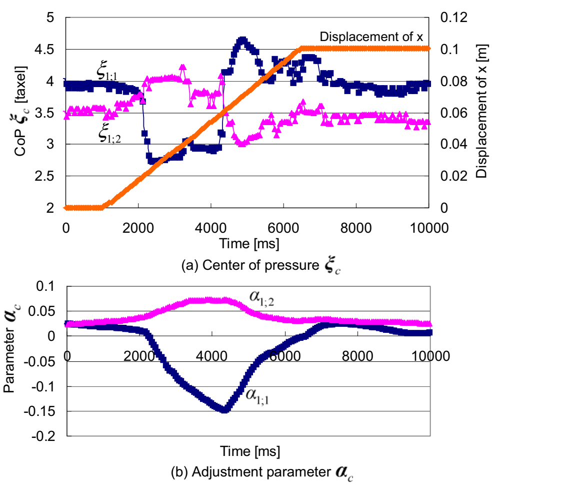


Fig. 13. Center of pressure $\boldsymbol{\xi}_c$ and adjustment parameter vector $\boldsymbol{\alpha}_c$ on the right forearm when tactile feedback was applied.

contact position was also activated to keep the object between the arms. The results for the right forearm are shown in Fig. 13. It can be seen that the position of the center of pressure $\boldsymbol{\xi}_1 = [\xi_{1;1}, \xi_{1;2}]^T$ changed during the movement of the object but recovered to that in the initial state because of tactile feedback. The adjustment parameter vector $\boldsymbol{\alpha}_1 = [\alpha_{1;1}, \alpha_{1;2}]^T$ is also shown. The tactile sensor output patterns at 0.5 s, 3.0 s, and 9.7 s are shown in Fig. 14, where the size of the squares indicates the magnitude of output from the sensing elements with a log scale.

## VII. Conclusion

We have proposed a whole-body contact manipulation method using tactile information for use with human-interactive robots. The method consists of the generation of a trajectory that depends on the contact positions, and sensor feedback to suppress deviations in actual situations.

We conducted experiments using our robot RIBA and obtained promising results, but we used an inanimate object without joints. After conducting experiments with a lifesize dummy, we will apply this method to real humans.

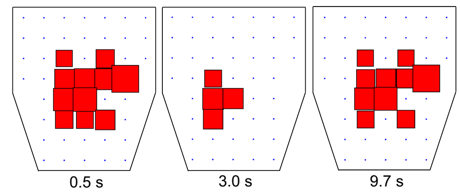


Fig. 14. Tactile sensor output patterns on the contacting surface of the right forearm when tactile feedback was activated.

## VIII. Acknowledgment


This research was supported in part by Grant-in-Aid for Scientific Research from Japan Society for the Promotion of Science.


## References


[1] My Spoon WEB page: http://www.secom.co.jp/english/myspoon/

[2] K. Wada, T. Shibata, T. Saito, and K. Tanie, "Psychological and Social Effects in Long-Term Experiment of Robot Assisted Activity to Elderly People at a Health Service Facility for the Aged," in *Proc. IEEE/RSJ International Conference on Intelligent Robots and Systems (IROS)*, pp.3068–3073, 2004.

[3] C. Mandel, T. Lüth, T. Laue, T. Röfer, A. Gräser, and B. Krieg-Brückner, "Navigating a Smart Wheelchair with a Brain-Computer Interface Interpreting Steady-State Visual Evoked Potentials," in *Proc. IEEE/RSJ International Conference on Intelligent Robots and Systems (IROS)*, pp.1118–1125, 2009.

[4] T. Hayashi, H. Kawamoto, and Y. Sankai, "Control Method of Robot Suit HAL Working as Operator's Muscle Using Biological and Dynamical Information," in *Proc. IEEE/RSJ International Conference on Intelligent Robots and Systems (IROS)*, pp.3455–3460, 2005.

[5] T. Mukai, S. Hirano, H. Nakashima, Y. Kato, Y. Sakaida, S. Guo, and S. Hosoe, "Development of a Nursing-Care Assistant Robot RIBA That Can Lift a Human in Its Arms," in *Proc. IEEE/RSJ International Conference on Intelligent Robots and Systems (IROS)*, pp.5996–6001, 2010.

[6] K. Salisbury, W. Townsend, B. Eberman, and D. DiPietro, "Preliminary Design of a Whole-Arm Manipulation System (WAMS)," in *Proc. IEEE International Conference on Robotics and Automation (ICRA)*, Vol. 1, pp.254–260, 1988.

[7] M. Kaneko, M. Higashimori, and T. Tsuji, "Transition Stability of Enveloped Objects," in *Proc. IEEE International Conference on Robotics and Automation (ICRA)*, pp.3040–3046, 1998.

[8] T. Watanabe, K. Harada, T. Yoshikawa, and Z. Jiang, "Towards Whole Arm Manipulation by Contact State Transition," in *Proc. IEEE/RSJ International Conference on Intelligent Robots and Systems (IROS)*, pp.5682–5687, 2006.

[9] K. Harada and M. Kaneko, "Whole Body Manipulation," in *Proc. IEEE International Conference on Robotics, Intelligent Systems and Signal Processing*, Vol. 1, pp.190–195, 2003.

[10] Y. Ohmura and Y. Kuniyoshi, "Humanoid Robot which can Lift a 30kg Box by Whole Body Contact and Tactile Feedback," in *Proc. IEEE/RSJ International Conference on Intelligent Robots and Systems (IROS)*, pp.1136–1141, 2007.

[11] S. Nozawa, R. Ueda, Y. Kakiuchi, K. Okasa, and M. Inaba, "A Full-Body Motion Control Method for a Humanoid Robot Based on On-Line Estimation of the Operational Force of an Object with an Unknown Weight," in *Proc. IEEE/RSJ International Conference on Intelligent Robots and Systems (IROS)*, pp.2684–2691, 2010.

[12] T. Mukai and Y. Kato, "1 ms Soft Areal Tactile Giving Robots Soft Response," *J. Robotics and Mechatronics*, Vol. 20, No. 3, pp.473–480, 2008.

[13] M.W. Spong and M. Vidyasagar, *Robot Dynamics and Control*, John Wiley & Sons, 1989.